Short Communication

Cure Kinetics of Samarium-doped Fe_3O_4/Epoxy Nanocomposites

Maryam Jouyandeh[a], Mohammad Reza Ganjali[a,b,c], Mehdi Mehrpooya[d], Otman Abida[e], Karam Jabbour[e], Navid Rabiee[f], Sajjad Habibzadeh[g], Amin Hamed Mashahdzadeh[h], Alberto García-Peñas[i,j], Florian J. Stadler[i], Mohammad Reza Saeb[k,*]

a Center of Excellence in Electrochemistry, School of Chemistry, University of Tehran, Tehran, 14176-14411, Iran; maryam.jouyande@gmail.com (M.J.) and ganjali@ut.ac.ir (M.R.G.)
b School of Resources and Environment, University of Electronic Science and Technology of China, Chengdu, 611731, China
c Biosensor Research Center, Endocrinology and Metabolism Molecular-Cellular Sciences Institute, Tehran University of Medical Sciences, Tehran, 14117-13137, Iran
d Department of Renewable Energies and Environment, Faculty of New Sciences and Technologies, University of Tehran, Tehran, Iran mehrpoya@ut.ac.ir (M.M.)
e College of Engineering and Technology, American University of the Middle East, Kuwait; otman.abida@aum.edu.kw (O.A.) and karam.jabbour@aum.edu.kw (K.J.)
f Department of Physics, Sharif University of Technology, Tehran, 11155-9161, Iran; nrabiee94@gmail.com (N.R.)
g Department of Chemical Engineering, Amirkabir University of Technology (Tehran Polytechnic), Tehran, 15916-34311, Iran; sajjad.habibzadeh@aut.ac.ir (S.H.)
h Mechanical and Aerospace Engineering, School of Engineering and Digital Sciences, Nazarbayev University, Nur-Sultan 010000, Kazakhstan; amin.hamed.m@gmail.com (A.H.M.)
i College of Materials Science and Engineering, Guangdong Research Center for Interfacial Engineering of Functional Materials, Nanshan District Key Laboratory for Biopolymers and Safety Evaluation, Shenzhen Key Laboratory of Polymer Science and Technology, Lihu Campus, Shenzhen University, Shenzhen 518055, China; alberto.garcia.penas@uc3m.es (A.G-P.) and fjstadler@szu.edu.cn (F.J.S.)
j Departamento de Ciencia e Ingeniería de Materiales e Ingeniería Química (IAAB), Universidad Carlos III de Madrid, 28911 Leganés, Madrid, Spain
k Department of Polymer Technology, Gdańsk University of Technology, G. Narutowicza 11/12 80-233, Gdańsk, Poland; mrsaeb2008@gmail.com (M.R.S.)

Abstract: There was a question on "how lanthanides doping in iron oxide affects cure kinetics of epoxy-based nanocomposites?" To answer, we synthesized samarium (Sm)-doped Fe_3O_4 nanoparticles via electrochemical method and characterized it using FTIR, XRD, FE-SEM, EDX, TEM, and XPS analyses. The magnetic particles were uniformly dispersed in epoxy resin to increase the curability of the epoxy/amine system. The effect of the lanthanide dopant on the curing reaction of epoxy with amine was explored by modeling DSC experimental data based on model-free methodology. It was found that Sm^{3+} in the structure of Fe_3O_4 crystal participates in cross-linking of epoxy by catalyzing the reaction between epoxide rings and amine groups of curing agents. In addition, the etherification reaction of active OH groups on the surface of nanoparticles reacts with epoxy rings which prolongs the reaction time at the late stage of reaction where diffusion is the dominant mechanism.

Keywords: Lanthanide; Samarium (Sm)-doped Fe_3O_4 nanoparticles; Epoxy coating; Anticorrosion; Curing reaction.

1. Introduction

Magnetic nanoparticles are a class of nanostructured materials of current interest, due largely to their advanced technological and medical applications, envisioned or realized [1]. Among the various magnetic nanoparticles under investigation, magnetite (Fe_3O_4) nanoparticles are arguably the most extensively studied [2]. Furthermore, with an

eye on possibly altering the structure and properties of the parent nanoparticles and creating multifunctional materials, doping of magnetite nanoparticles with other metal ions has been explored.

Lanthanide ions (Ln) are an interesting class of dopants with unique optical and magnetic properties associated with their f-electronic configurations [3]. In addition, the doped particles so prepared have been found to possess physical and chemical characteristics not significantly different from the parent, undoped magnetite nanoparticles. The doping of other metals/metal ions, such as zinc, manganese, copper, nickel, and cobalt, into the Fe_3O_4 enhances the availability of its surface sites [4-6].

In the present study, samarium (Sm)-doped Fe_3O_4 nanoparticles were fabricated via an electrochemical method. The synthesized samples were well characterized by FTIR, XRD, FE-SEM, EDX, TEM, and XPS. Then, the epoxy-based film was reinforced with Ce-doped Fe_3O_4 nanoparticles to obtain an excellent corrosion protection coating. The cure potential of the epoxy-containing Sm-doped Fe_3O_4 nanoparticles was evaluated with dynamic differential calorimetry (DSC) at different heating rates of 2.5, 5, 7.5, and 10 °C/min.

2. Materials and Methods

Iron (II) chloride ($FeCl_2{\cdot}4H_2O$), iron(III) nitrate nonahydrate 99.9% ($Fe(NO_3)_3{\cdot}9H_2O$), and Samarium(III) nitrate ($Sm(NO_3)_3{\cdot}(H_2O)_2$) were supplied by Sigma-Aldrich. Araldite LY 5052 epoxy resin and HY 5052 curing agent were purchased from MIS Hindustan Ciba-Geigy.

2.2. Synthesis of Sm-doped Fe_3O_4 nanoparticles

Sm^{3+}-doped Fe_3O_4 nanoparticles were prepared through the cathodic electrodeposition (CED) procedure using a stainless steel cathode (316L, 5 cm × 5 cm × 0.5 mm) inside two graphite anodes. The electrolyte 0.005 molar solution of Iron(III) nitrate nonahydrate (2 g), Iron (II) Chloride (1 g) and Samarium(III) nitrate (0.6 g) was prepared in water. Then, deposition was occurred using Potentiostat/Galvanostat, Model: NCF-PGS 2012, Iran at 25 °C and current density of 10 mA cm^{-2} for 30 min followed by rinsing with deionized water several times. Eventually, the dispersed Sm-Fe_3O_4 deposit in deionized water centrifuged at 6000 rpm for 20 min, separated and dried at 70 °C for 1 h.

2.3. Preparation of epoxy/Sm-doped Fe_3O_4 nanocomposite

Epoxy nanocomposites was obtained by mixing 0.1 wt.% of Sm-doped Fe_3O_4 using a mechanical mixer at 2500 rpm for 15 min. Then, Sm-doped Fe_3O_4 in epoxy further mixed by sonication for 5 min. Finally, the curing agent was added to EP/Sm-Fe_3O_4 nanocomposite in the stoichiometric ratio of 38/100 (curing agent/epoxy).

2.4. Characterization

The FTIR spectrum of Sm-doped Fe_3O_4 nanoparticles was obtained by Bruker Vector spectrometer, Coventry, UK, between 4000–400 cm^{-1} wavelength. X-ray diffraction (XRD) of nanoparticles was performed by PW-1800 apparatus (Amsterdam, Netherlands) with Co Kα radiation. The micro- and nano-images of Sm-Fe_3O_4 nanoparticles were obtained by FESEM and EDX-Mapping (Mira 3-XMU) at the voltage of 100 kV and TEM (Zeiss-EM10C-80 kV, Germany). XPS elemental analysis of Sm-Fe_3O_4 nanoparticles was analyzed by a Thermo Fisher Scientific instrument.

The cure reaction of neat epoxy and EP/Sm-Fe_3O_4 nanocomposite investigated by DSC (Perkin Elmer, DSC 4000, Waltham, MA, USA) at four different heating rates (2.5, 5, 7.5 and 10 °C·min^{-1}).

3. Results and discussion

 doi:10.20944/preprints202112.0102.v1

3.1. Characterization of Sm–Fe_3O_4 nanoparticles

The FTIR spectrum of the prepared Sm–Fe_3O_4 nanoparticle is shown in Fig. 1(a). Two sharp bands can be observed at 562 cm^{-1} and 628 cm^{-1} which is ascribed to the splitting of the ν1 band of the Fe–O. A wide peak in the range of 415–443 cm^{-1} is because of ν2 band of the Fe–O and Sm–O [7]. Appearance of bands at 1648 and 3325 cm^{-1} are attributed to the stretching and deformation vibrations of O–H groups on the surface of Sm–Fe_3O_4 nanoparticle.

Figure 1(b) shows the XRD pattern of Sm-Fe_3O_4 nanoparticles, which the cubic spinel structure of Magnetite Fe_3O_4 [Joint Committee on Powder Diffraction Standards (JCPDS) 76-1849 and Inorganic Crystal Structural Database (ICSD) 28664]. A significant change was not observed in the XRD patterns of doped nanoparticles. The XRD pattern shows that doping Sm does not change the crystal structure of Fe_3O_4 nanoparticles.

The oxygen atoms in magnetite (Fe_3O_4) form a close-packed face-centered cubic sublattice with Fe(II) located in octahedral sites and with Fe(III) equally distributed in octahedral and tetrahedral sites (inverse Spinel structure) [8]. The cubic unit cell contains eight formula units and can be denoted as $(Fe_8^{3+})^{tetr}[Fe^{3+}Fe^{2+}]_8{}^{oct}O_{32}$. Along the (111) axis, the oxygen layers are cubic close-packed. Transition metals can occupy either one of these sites [9]. On the other hand, lanthanide(III) ions exhibit distorted six coordination sites or face-capped octahedral seven coordination sites in the Ln_2O_3 crystal structure [10]. Therefore, in the present case, lanthanide(III) ions may occupy some of the octahedral sites in the Fe_3O_4 inverse Spinel structure.

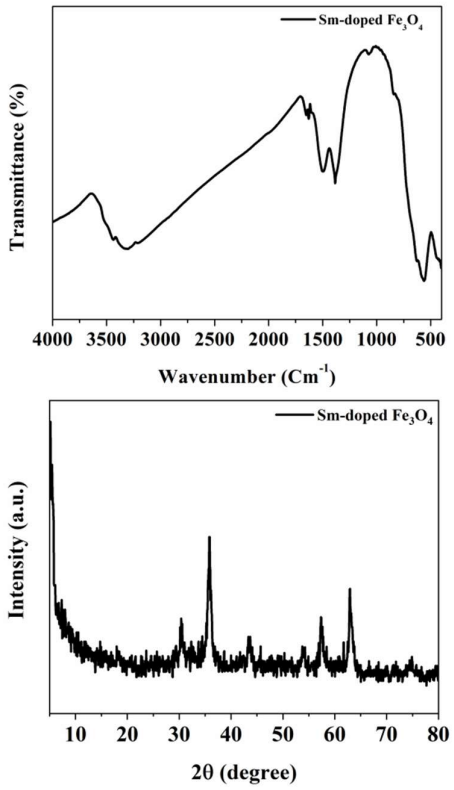

Fig. 1. (a) FTIR spectra of Ce-doped Fe_3O_4 and (b) XRD pattern of Sm-doped Fe_3O_4

Figure 2 shows the FESEM, EDS, mapping, and TEM images of Sm-Fe_3O_4 nanoparticles. The average particle size is about 20 nm. EDX experiments were performed to confirm the presence of both Fe and Sm in the nanoparticles, as shown in Figure 2 (b). The presence of Sm and Fe is obvious in addition to the peaks corresponding to O and Au. Au stems from the TEM grids used for the analysis and the surfactant molecules.

 doi:10.20944/preprints202112.0102.v1

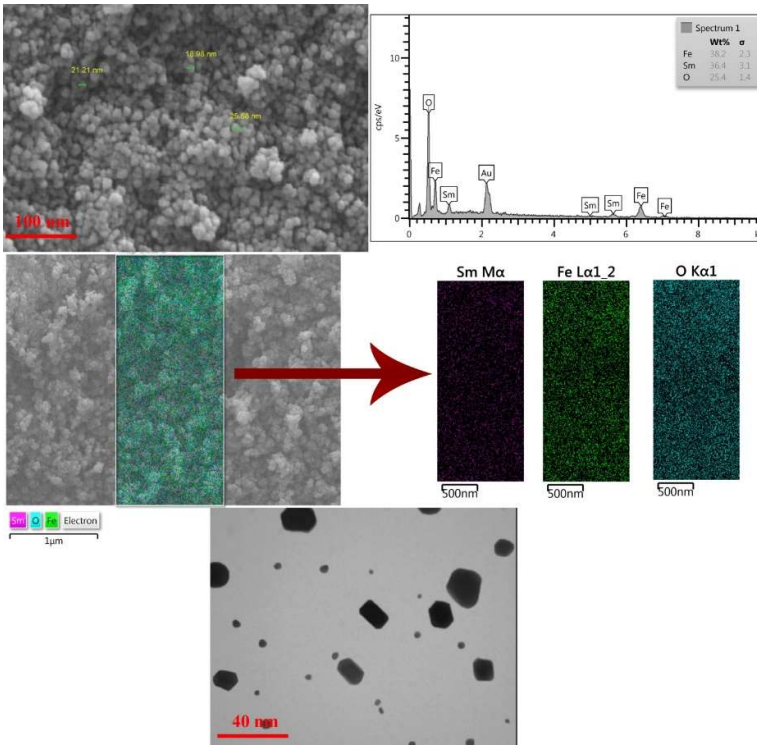

Fig. 2. (a) FESEM, (b) EDX, (c) elemental mapping and (d) TEM of Sm-doped Fe_3O_4

XPS analysis confirms the presence of Fe and Sm, O, and C in the Sm-Fe_3O_4 nanoparticles (Figure 3(a)). The Fe2p peaks in the XPS spectrum of Sm-Fe_3O_4 nanoparticles (Figure 3(b)) show the $Fe2p_{1/2}$ and $Fe2p_{3/2}$ peaks at around 710 and 720 eV, respectively, which confirm the presence of Fe(III) [11]. The $Fe2p_{1/2}$ peak with a shoulder at 708 eV and $Fe2p_{3/2}$ peak with a shoulder at 721 eV indicates the presence of Fe(II) in Fe_3O_4 [12].

Sm-$3d_{5/2}$ regions of Sm-Fe_3O_4 nanoparticles are shown in Figure 3(c). By evaluating the binding energy values ($3d_{5/2}$) of Sm(III) (1079 and 1107 eV) present in the nanoparticles with their standards [Sm_2O_3 (1082 and 1108 eV) [13], it can be concluded that this lanthanide is present in its +3 oxidation states in the nanoparticles. Subtle changes observed may be due to the different coordination environments occupied in the crystal structure as observed by others in other europium-oxo compounds.

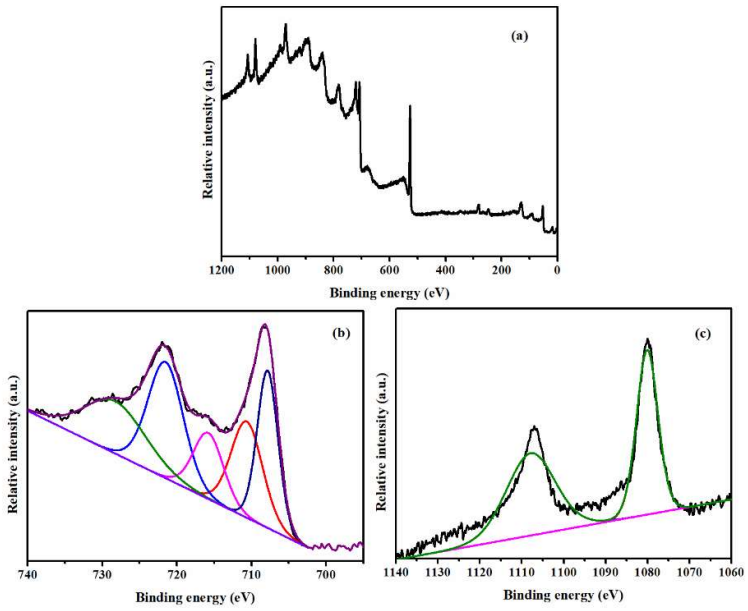

Fig.3. XPS spectra of the Sm-doped Fe_3O_4 (a) Survey, (b) Fe2p and (c) Sm3d.

3.2. Curing analysis

Figure 4 displays nonisothermal DSC thermographs of neat epoxy and EP/Sm-Fe_3O_4 cured with a stoichiometric amount of amine curing agent at heating rates of 2.5, 5, 7.5, and 10 °C/min. One exothermic peak can be observed for both samples at different heating rates, which revealed that the presence of Sm-Fe_3O_4 nanoparticles in the epoxy matrix does not change the domination of the chemically controlled reaction mechanism [14,15].

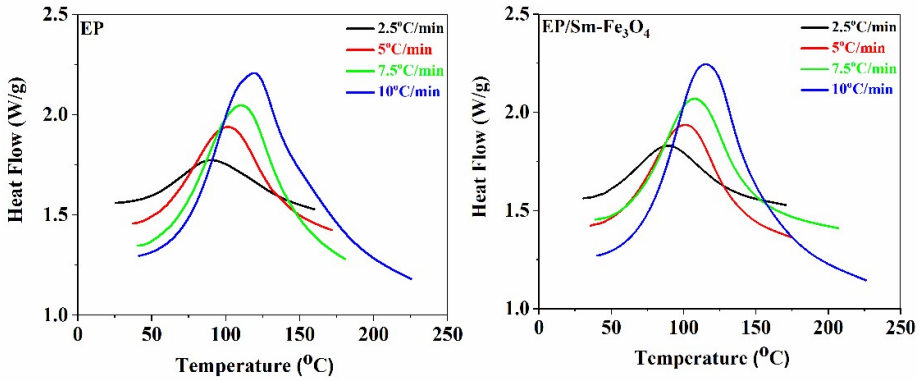

Fig.4. Dynamic DSC thermograms of EP and EP/Sm-Fe3O4 at different heating rates.

The Cure characteristics of EP and EP/Sm-Fe_3O_4 nanocomposite include T_{Onset}, T_{Endset}, T_P, ΔT, and ΔH_∞ , which are the onset, endset, the exothermal peak temperature, temperature interval, and the enthalpy of complete cure, respectively, are reported in Table 1. T_{Onset}, T_{Endset}, and T_P shifted towards elevated temperatures by increasing heating rates from 2.5 to 10 °C/min to compensate for reducing curing time [16,17].

The addition of Sm-Fe_3O_4 nanoparticles decreased T_{Onset} and T_P of epoxy/amine reaction, indicating that Sm doped magnetic nanoparticles accelerate cross-linking reaction. The surface activity of Sm-Fe_3O_4 nanoparticles can ascribe this increment in the system's reactivity due to the presence of Sm^{3+} in the crystal structure of nanoparticles

that catalyze the reaction between epoxy and amine curing agents [4,18]. However, T_{Endset}, ΔT increased for EP/Sm-Fe_3O_4 nanocomposite compared to neat epoxy, which means that at the late stage of cure reaction, the OH groups on the surface of nanoparticles participate in etherification reaction and prolong the cross-linking of epoxy reaction.

The effect of etherification reaction of OH groups on the surface of Sm-Fe_3O_4 nanoparticles besides the catalyzing effect of Sm^{3+}, which acts as Lewis acid increase total heat of cure (ΔH_∞) of EP/Sm-Fe_3O_4 nanocomposite in comparison to neat epoxy [19].

Table 1. Cure characteristics of EP and EP/Sm-Fe_3O_4 nanocomposite as a function of heating rate.

Sample	Heating rate (°C/min)	T_{Onset} (°C)	T_p (°C)	T_{Endset} (°C)	ΔT(°C)	ΔH_∞(J/g)	ΔT^*	ΔH^*	*CI*
EP	2.5	25.71	90.367	159.93	134.22	329.62	N.a.	N.a.	N.a.
	5.0	37.37	101.69	171.72	134.35	336.21	N.a.	N.a.	N.a.
	7.5	40.65	110.28	180.68	140.03	344.05	N.a.	N.a.	N.a.
	10	41.43	119.15	225.3	183.87	404.33	N.a.	N.a.	N.a.
EP/Sm-Fe_3O_4	2.5	30.8	89.407	170.6	139.8	385.77	1.04	1.17	1.22
	5.0	35.69	101.5	175.2	139.51	363.72	1.04	1.08	1.12
	7.5	39.13	107.66	207.02	167.89	296.34	1.2	0.86	1.03
	10	40.1	115.14	225.97	185.87	403.44	1.01	1.01	1.02
N.a.: Not applicable									

The effect of curability of Sm-Fe_3O_4 nanoparticles in epoxy/amine system are specified by Cure Index:

$$CI = \Delta T^* \times \Delta H^*, \quad \Delta T^* = \frac{\Delta T_{nanocomposite}}{\Delta T_{\mathrm{Re}\,ference}} \quad and \quad \Delta H^* = \frac{\Delta H_{nanocomposite}}{\Delta H_{\mathrm{Re}\,ference}}, \tag{1}$$

ΔT is temperature window within which curing occurs, with subscripts of "nanocomposite" and "Reference" for nanocomposite and blank epoxy systems, respectively. Similarly, ΔH_∞ of such systems are defined. The asterisk terms in each case are dimenshionless. *Good*, *Poor*, and *Excellent* curing reaction of nanocomposites occurs at CI>ΔH*, CI < ΔT*, and ΔT* < CI < ΔH*, respectively. The addition of Sm-Fe_3O_4 nanoparticles in the epoxy matrix resulted in a *Good* cure reaction, which means that Sm^{3+} participates in cross-linking of epoxy by catalyzing the reaction between epoxide rings and amine groups of curing agents. In addition, the active OH groups on the surface of nanoparticles react with epoxy polar groups that increase both ΔT and ΔH and result in *Good* CI.

Figure 5 shows the conversion (α) of curing reaction as a function of temperature which obtained from Eq. 2:

$$\alpha = \frac{\Delta H_T}{\Delta H_\infty}, \tag{2}$$

where ΔH_T is the enthalpy of reaction at a specific temperature.

In the initial stage of the curing reaction, cross-linking occurs rapidly until reaching gel point under the control of chemical reaction between the epoxy ring and amine groups of curing agent. By contrast, at the late stage of cure, where diffusion is dominant, the cross-linking occurs slowly. Also, Sm-Fe_3O_4 nanoparticles accelerate cross-linking of epoxy after vitrification which indicated an acceleration of diffusion mechanisms due to the presence of OH groups on the surface of nanoparticles [20].

Preprints (www.preprints.org) | NOT PEER-REVIEWED | Posted: 7 December 2021 doi:10.20944/preprints202112.0102.v1

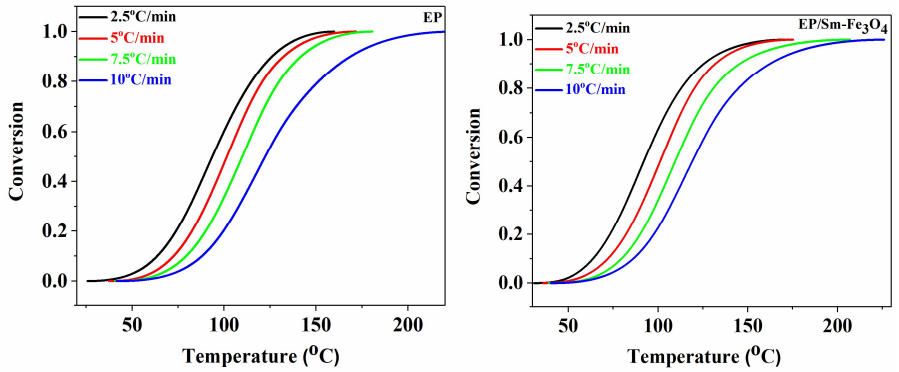

Fig. 5. The fractional extent of conversion as a function of reaction time for EP and EP/Sm-Fe_3O_4 nanocomposite at heating rates of 2.5, 5, 7.5, and 10 °C/min.

Isoconversional model-free Friedman and Kissinger-Akahira-Sunose (KAS) were employed to obtain the apparent activation energy (E_α) of curing reaction (Supporting Information, Eqs. S1 and S2, Figures S1 and S2) [21,22]. The apparent activation energy of neat epoxy and EP/Sm-Fe_3O_4 nanocomposite as a function of α based on both Friedman and KAS are shown in Figure 6. E_α reduced for neat epoxy and its nanocomposite in α higher than 0.5 due to the participation of OH groups in epoxide ring-opening at a later stage of curing reaction revealing the autocatalytic mechanism of epoxy cure reaction [23,24]. The higher E_α values for EP/Sm-Fe_3O_4 nanocomposite compared to neat epoxy can be attributed to the higher viscosity of the epoxy system in the presence of Sm-Fe_3O_4 nanoparticles [25].

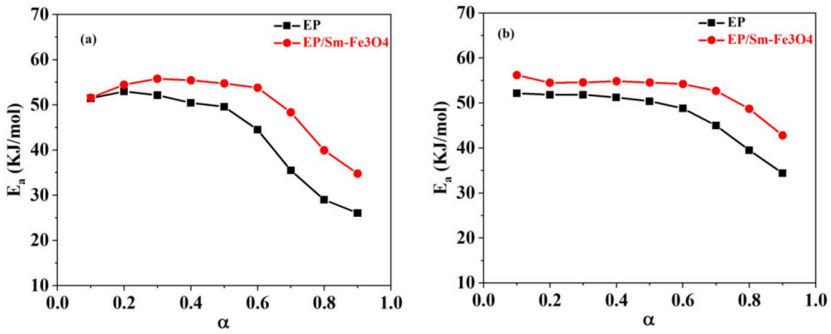

Fig. 6. Evolution of activation energy for EP and EP/Sm-Fe_3O_4 nanocomposite estimated by (a) differential Friedman model and (b) integral KAS model.

The autocatalytic reaction model ($f(\alpha)$, Eq. 3) of neat epoxy and its nanocomposite was obtained by Friedman and Malek model (Supporting Information, Eqs. S2-S5, Figures S3 and S4).

$$f(\alpha) = \alpha^m (1-\alpha)^n, \quad (3)$$

The reaction model parameters, including the pre-exponential factor (lnA), non-catalytic (n), and autocatalytic (m) reaction orders, were determined from Eqs. S6 and S7 and Figs. S5 and S6 and reported in Table 2. As can be observed, both n and m increased for EP/Sm-Fe_3O_4 nanocomposite compared to neat epoxy. Increment of n indicated the catalyzing effect of Sm^{3+} as a Lewis acid in the reaction between the epoxy ring and amine curing agent and enhancement of m is because of reaction of OH groups on the surface of Sm-Fe_3O_4 nanoparticles with epoxide rings. The retardation effect Sm-Fe_3O_4 nanoparticles on cure reaction of epoxy is reflected in higher lnA values.

Table 2. The kinetic parameters evaluated for the curing of EP and EP/Sm-Fe_3O_4 nanocomposite based on Friedman and KAS models at different heating rates.

Designation	Heating rate (°C/min)	*Friedman*			*KAS*		
		m	*n*	*lnA* (s^{-1})	*m*	*n*	*lnA* (s^{-1})
EP	2.5	0.14	1.32	12.09	0.09	1.36	13.3
	5.0	0.29	1.38	12.71	0.24	1.42	13.9
	7.5	0.29	1.36	12.76	0.24	1.4	13.92
	10	0.25	1.69	12.57	0.2	1.74	13.71
EP/Sm-Fe_3O_4	2.5	0.16	1.58	14.5	0.13	1.62	15.39
	5.0	0.23	1.47	14.8	0.20	1.5	15.66
	7.5	0.34	1.72	15.05	0.30	1.75	15.9
	10	0.31	1.85	14.9	0.28	1.89	15.73

The validation of isoconversional methods (Friedman and KAS) are obtained by comparison with the experimental data and shown in Fig. 7. Clearly, both KAS and Friedman approaches can predict the curing rate of cross-linking reaction for neat epoxy and Sm-Fe_3O_4 nanoparticles incorporated epoxy system.

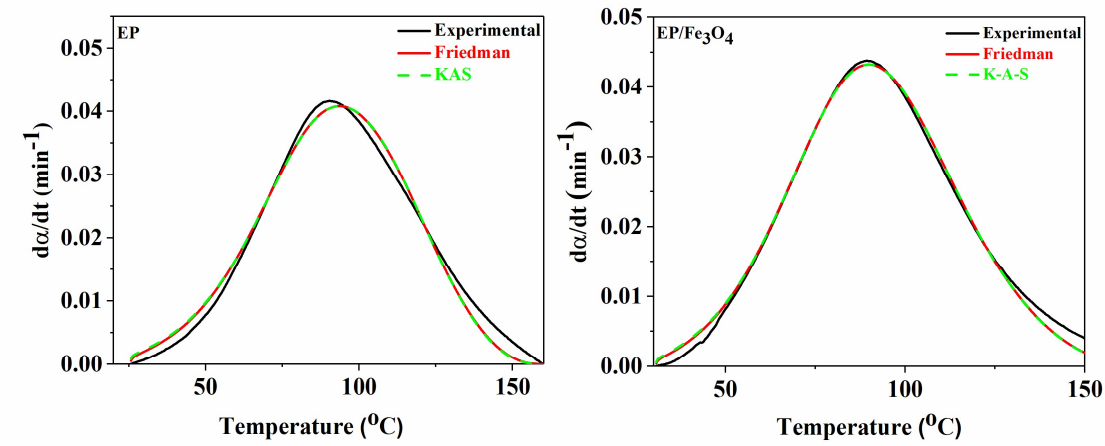

Fig. 7. Comparison of experimental data with the kinetic models for EP and EP/Sm-Fe_3O_4 nanocomposite based on Friedman and KAS model.

5. Conclusions

Sm-doped Fe_3O_4 nanoparticle was synthesized through electrochemical method to investigate its effect on curability of Epoxy/amine system. XPS results indicated that samarium is present in its +3 oxidation states in the structure of Fe_3O_4 lattice. The XRD pattern revealed that Sm^{3+} ions occupy the octahedral sites in the Fe_3O_4 crystal structure. DSC analysis at different heating rate showed that addition of Sm-Fe_3O_4 nanoparticles accelerate cross-linking reaction due to the catalyzing effect of Sm^{3+} in the crystal structure of Fe_3O_4 nanoparticles on the reaction between epoxy and amine curing agent which reflected in lower T_{Onset} and T_P. Obtaining Good CI by addition of Sm-Fe_3O_4 nanoparticles in epoxy matrix showed that Sm^{3+} participate in cross-linking of epoxy by catalyzing the reaction between epoxide rings and amine groups of curing agent and etherification reaction of active OH groups on the surface of nanoparticles reacts with epoxy rings. The apparent activation energy that determined by isoconversional Friedman and KAS methods indicated complex curing reaction of epoxy in the presence of Sm-Fe_3O_4 nano-

particles which cause increment of average Eα value from 47.3 for neat epoxy to 52.6 kJ/mol. The autocatalytic reaction model was validated by experimental data.

Supplementary Materials: The Supplementary Materials are available online at www.mdpi.com.

Author Contributions: Conceptualization, M.R.S.; methodology, M.J. and M.R.G.; software, M.J.; validation, M.J., and M.R.S.; formal analysis, M.R. and O.A.; investigation, K.J. and N.R.; data curation, S.H. and A.H.M.; writing—original draft preparation, M.J.; writing—review and editing, A.G-P., F.J.S., and M.R.S.; visualization, M.J. and M.R.S..; supervision, M.R.S.; project administration, M.R.G.; All authors have read and agreed to the published version of the manuscript.

Funding: This research received no external funding.

Conflicts of Interest: The authors declare no conflict of interest.

References

1. Yavuz, C.T.; Mayo, J.; William, W.Y.; Prakash, A.; Falkner, J.C.; Yean, S.; Cong, L.; Shipley, H.J.; Kan, A.; Tomson, M. Low-field magnetic separation of monodisperse Fe3O4 nanocrystals. *science* **2006**, *314*, 964-967.
2. Roca, A.; Morales, M.; O'Grady, K.; Serna, C. Structural and magnetic properties of uniform magnetite nanoparticles prepared by high temperature decomposition of organic precursors. *Nanotechnology* **2006**, *17*, 2783.
3. Groman, E.V.; Bouchard, J.C.; Reinhardt, C.P.; Vaccaro, D.E. Ultrasmall mixed ferrite colloids as multidimensional magnetic resonance imaging, cell labeling, and cell sorting agents. *Bioconjugate chemistry* **2007**, *18*, 1763-1771.
4. Jouyandeh, M.; Ali, J.A.; Aghazadeh, M.; Formela, K.; Saeb, M.R.; Ranjbar, Z.; Ganjali, M.R. Curing epoxy with electrochemically synthesized ZnxFe3-xO4 magnetic nanoparticles. *Progress in Organic Coatings* **2019**, *136*, 105246, doi:https://doi.org/10.1016/j.porgcoat.2019.105246.
5. Jouyandeh, M.; Ali, J.A.; Akbari, V.; Aghazadeh, M.; Paran, S.M.R.; Naderi, G.; Saeb, M.R.; Ranjbar, Z.; Ganjali, M.R. Curing epoxy with polyvinylpyrrolidone (PVP) surface-functionalized MnxFe3-xO4 magnetic nanoparticles. *Progress in Organic Coatings* **2019**, *136*, 105247, doi:https://doi.org/10.1016/j.porgcoat.2019.105247.
6. Jouyandeh, M.; Ganjali, M.R.; Ali, J.A.; Aghazadeh, M.; Karimzadeh, I.; Formela, K.; Colom, X.; Cañavate, J.; Saeb, M.R. Curing epoxy with ethylenediaminetetraacetic acid (EDTA) surface-functionalized CoxFe3-xO4 magnetic nanoparticles. *Progress in Organic Coatings* **2019**, *136*, 105248, doi:https://doi.org/10.1016/j.porgcoat.2019.105248.
7. Aghazadeh, M.; Ganjali, M.R. Samarium-doped Fe 3 O 4 nanoparticles with improved magnetic and supercapacitive performance: a novel preparation strategy and characterization. *Journal of Materials Science* **2018**, *53*, 295-308.
8. Ketteler, G.; Weiss, W.; Ranke, W.; Schlögl, R. Bulk and surface phases of iron oxides in an oxygen and water atmosphere at low pressure. *Physical Chemistry Chemical Physics* **2001**, *3*, 1114-1122.
9. Kim, T.Y.; Lee, M.S.; Kim, Y.I.; Lee, C.-S.; Park, J.C.; Kim, D. The enhanced anisotropic properties of the Fe3− xMxO4 (M= Fe, Co, Mn) films deposited on glass surface from aqueous solutions at low temperature. *Journal of Physics D: Applied Physics* **2003**, *36*, 1451.
10. Cotton, S. *Lanthanide and actinide chemistry*; John Wiley & Sons: 2013.
11. Kataby, G.; Ulman, A.; Cojocaru, M.; Gedanken, A. Coating a bola-amphiphile on amorphous iron nanoparticles. *Journal of Materials Chemistry* **1999**, *9*, 1501-1506.
12. Tie, S.-L.; Lee, H.-C.; Bae, Y.-S.; Kim, M.-B.; Lee, K.; Lee, C.-H. Monodisperse Fe3O4/Fe@ SiO2 core/shell nanoparticles with enhanced magnetic property. *Colloids and Surfaces A: Physicochemical and Engineering Aspects* **2007**, *293*, 278-285.
13. De Silva, C.R.; Smith, S.; Shim, I.; Pyun, J.; Gutu, T.; Jiao, J.; Zheng, Z. Lanthanide (III)-doped magnetite nanoparticles. *Journal of the American Chemical Society* **2009**, *131*, 6336-6337.
14. Jouyandeh, M.; Tikhani, F.; Shabanian, M.; Movahedi, F.; Moghari, S.; Akbari, V.; Gabrion, X.; Laheurte, P.; Vahabi, H.; Saeb, M.R. Synthesis, characterization, and high potential of 3D metal–organic framework (MOF) nanoparticles for curing with epoxy. *Journal of Alloys and Compounds* **2020**, *829*, 154547, doi:https://doi.org/10.1016/j.jallcom.2020.154547.

15. Karami, Z.; Jouyandeh, M.; Ali, J.A.; Ganjali, M.R.; Aghazadeh, M.; Maadani, M.; Rallini, M.; Luzi, F.; Torre, L.; Puglia, D., et al. Cure Index for labeling curing potential of epoxy/LDH nanocomposites: A case study on nitrate anion intercalated Ni-Al-LDH. *Progress in Organic Coatings* **2019**, *136*, 105228, doi:https://doi.org/10.1016/j.porgcoat.2019.105228.
16. Jouyandeh, M.; Ganjali, M.R.; Ali, J.A.; Aghazadeh, M.; Stadler, F.J.; Saeb, M.R. Curing epoxy with electrochemically synthesized NixFe3-xO4 magnetic nanoparticles. *Progress in Organic Coatings* **2019**, *136*, 105198, doi:https://doi.org/10.1016/j.porgcoat.2019.06.044.
17. Jouyandeh, M.; Zarrintaj, P.; Ganjali, M.R.; Ali, J.A.; Karimzadeh, I.; Aghazadeh, M.; Ghaffari, M.; Saeb, M.R. Curing epoxy with electrochemically synthesized GdxFe3-xO4 magnetic nanoparticles. *Progress in Organic Coatings* **2019**, *136*, 105245, doi:https://doi.org/10.1016/j.porgcoat.2019.105245.
18. Jouyandeh, M.; Karami, Z.; Ali, J.A.; Karimzadeh, I.; Aghazadeh, M.; Laoutid, F.; Vahabi, H.; Saeb, M.R.; Ganjali, M.R.; Dubois, P. Curing epoxy with polyethylene glycol (PEG) surface-functionalized NixFe3-xO4magnetic nanoparticles. *Progress in Organic Coatings* **2019**, *136*, 105250, doi:https://doi.org/10.1016/j.porgcoat.2019.105250.
19. Jouyandeh, M.; Ganjali, M.R.; Ali, J.A.; Aghazadeh, M.; Stadler, F.J.; Saeb, M.R. Curing epoxy with electrochemically synthesized MnxFe3-xO4 magnetic nanoparticles. *Progress in Organic Coatings* **2019**, *136*, 105199, doi:https://doi.org/10.1016/j.porgcoat.2019.06.045.
20. Tikhani, F.; Moghari, S.; Jouyandeh, M.; Laoutid, F.; Vahabi, H.; Saeb, M.R.; Dubois, P. Curing Kinetics and Thermal Stability of Epoxy Composites Containing Newly Obtained Nano-Scale Aluminum Hypophosphite (AlPO2). *Polymers* **2020**, *12*, 644.
21. Sbirrazzuoli, N.; Vyazovkin, S. Learning about epoxy cure mechanisms from isoconversional analysis of DSC data. *Thermochimica Acta* **2002**, *388*, 289-298.
22. Sbirrazzuoli, N.; Vyazovkin, S.; Mititelu, A.; Sladic, C.; Vincent, L. A study of epoxy - amine cure kinetics by combining isoconversional analysis with temperature modulated DSC and dynamic rheometry. *Macromol. Chem. Phys.* **2003**, *204*, 1815-1821.
23. Jouyandeh, M.; Jazani, O.M.; Navarchian, A.H.; Shabanian, M.; Vahabi, H.; Saeb, M.R. Surface engineering of nanoparticles with macromolecules for epoxy curing: Development of super-reactive nitrogen-rich nanosilica through surface chemistry manipulation. *Applied Surface Science* **2018**, *447*, 152-164, doi:https://doi.org/10.1016/j.apsusc.2018.03.197.
24. Jouyandeh, M.; Jazani, O.M.; Navarchian, A.H.; Shabanian, M.; Vahabi, H.; Saeb, M.R. Bushy-surface hybrid nanoparticles for developing epoxy superadhesives. *Applied Surface Science* **2019**, *479*, 1148-1160, doi:https://doi.org/10.1016/j.apsusc.2019.01.283.
25. Jouyandeh, M.; Paran, S.M.R.; Shabanian, M.; Ghiyasi, S.; Vahabi, H.; Badawi, M.; Formela, K.; Puglia, D.; Saeb, M.R. Curing behavior of epoxy/Fe3O4 nanocomposites: A comparison between the effects of bare Fe3O4, Fe3O4/SiO2/chitosan and Fe3O4/SiO2/chitosan/imide/phenylalanine-modified nanofillers. *Progress in Organic Coatings* **2018**, *123*, 10-19, doi:https://doi.org/10.1016/j.porgcoat.2018.06.006.